Journal of proteome research

pubs.acs.org/jpr

Article

Offline Two-Dimensional Liquid Chromatography–Mass Spectrometry for Deep Annotation of the Fecal Metabolome Following Fecal Microbiota Transplantation

Brady G. Anderson, Alexander Raskind, Rylan Hissong, Michael K. Dougherty, Sarah K. McGill, Ajay S. Gulati, Casey M. Theriot, Robert T. Kennedy, and Charles R. Evans*

Cite This: *J. Proteome Res.* 2024, 23, 2000–2012

Read Online

ACCESS | Metrics & More | Article Recommendations | Supporting Information

ABSTRACT: Biological interpretation of untargeted LC-MS-based metabolomics data depends on accurate compound identification, but current techniques fall short of identifying most features that can be detected. The human fecal metabolome is complex, variable, incompletely annotated, and serves as an ideal matrix to evaluate novel compound identification methods. We devised an experimental strategy for compound annotation using multidimensional chromatography and semiautomated feature alignment and applied these methods to study the fecal metabolome in the context of fecal microbiota transplantation (FMT) for recurrent *C. difficile* infection. Pooled fecal samples were fractionated using semipreparative liquid chromatography and analyzed by an orthogonal LC-MS/MS method. The resulting spectra were searched against commercial, public, and local spectral libraries, and annotations were vetted using retention time alignment and prediction. Multidimensional chromatography yielded more than a 2-fold improvement in identified compounds compared to conventional LC-MS/MS and successfully identified several rare and previously unreported compounds, including novel fatty-acid conjugated bile acid species. Using an automated software-based feature alignment strategy, most metabolites identified by the new approach could be matched to features that were detected but not identified in single-dimensional LC-MS/MS data. Overall, our approach represents a powerful strategy to enhance compound identification and biological insight from untargeted metabolomics data.

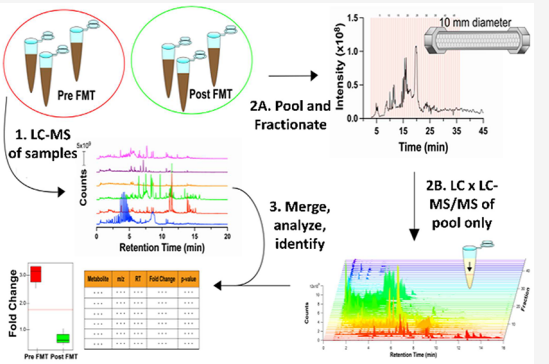

KEYWORDS: *Clostridioides difficile, C. diff, HILIC, RPLC, LC × LC, untargeted metabolomics, compound identification, bile acids, LC-MS, MS/MS*

INTRODUCTION

Untargeted metabolomics data typically contains hundreds to thousands of unknown features, even after data cleaning techniques are applied to reduce degenerate signals[1−4] and the best currently available spectral searching strategies are applied to identify metabolites.[5−7] The most important experimental method to help identify or annotate biologically relevant unknown metabolites is the acquisition of high-quality tandem mass spectrometry (MS/MS) data, which can be queried against experimental and *in-silico* spectral databases.[5] Yet even using multiple spectral libraries containing thousands of high-quality spectra, some features are inherently difficult to identify for one of several reasons: they may be present at low abundance and generate a poor quality MS/MS spectrum, the MS/MS spectra they produce may contain few unique product ions, they may be difficult to distinguish from structurally similar compounds that produce nearly identical spectra, or they may be confounded by chimeric MS/MS spectra resulting from cofragmentation of coeluting precursors with the same nominal mass.[6,7] Spectral resolution and mass accuracy also affect identification accuracy. Liquid chromatography (LC) can separate isomers, reduce competition for ionization and improve MS signal, but many features remain challenging to identify by data-dependent or data-independent LC-MS/MS due to incomplete chromatographic resolution or low abundance.[8] Ion mobility spectrometry-mass spectrometry has been proposed as a strategy to resolve isomers and measure collisional cross-section (CCS) values of small molecules.[9] However, recent work by Asef et al. demonstrated that comparing experimentally measured CCS against

Received: January 12, 2024
Revised: April 5, 2024
Accepted: May 10, 2024
Published: May 16, 2024

predicted values filtered fewer than 1/3 of candidate structures in a study involving *C. elegans* metabolites and lipids.[10]

Enhancing chromatographic separations is an additional strategy to improve compound identification performance in metabolomics. Current untargeted metabolomics studies commonly use relatively short chromatographic gradients (~20 min or less) to achieve sufficient throughput for large numbers of samples. For accurate quantification, sample loading quantities must avoid column or detector saturation for the most abundant features. However, these conditions are not optimized for compound identification. Previously, our group demonstrated significant improvement in compound identification performance when longer run times (~3 h), higher sample loading, and multirun precursor ion exclusion were used.[11] Such conditions only needed to be used to analyze a representative pooled sample, since software tools could be used to achieve confident alignment of newly identified compounds with features detectable but not identifiable using conventional LC-MS conditions.[12] However, at the longest gradients and highest loading conditions, broader peaks and increased coelution resulted in a leveling-off of the number of compounds identified in a sample, suggesting that a practical limit exists for one-dimensional (1D) LC separations using commercially available instrumentation and columns.

Larger diameter columns offer higher loading capacity than the 1 to 2.1 mm inner diameter columns typically used for LC-MS, but since electrospray ionization (ESI) sensitivity is mostly concentration-dependent,[13] higher mass loading can only be translated to improved sensitivity when eluted compounds can be concentrated before data acquisition by the MS.[14] By performing a separation using a semipreparative column (10 mm or larger bore), collecting and concentrating fractions, and reinjecting them on a narrower-bore column, higher mass loading can be achieved for many compounds while avoiding column overloading resulting in peak broadening. This technique, termed offline two-dimensional chromatography (LC × LC), also reduces coelution and corresponding ion suppression.[15] Only a few metabolomics-focused examples of LC × LC are found in the literature. In one such study, a semipreparative ion-pairing RPLC first dimension separation detected 3564 unique ion pairs in human urine after collected fractions were isotopically dansylated to impart additional hydrophobicity prior to an analytical scale RPLC separation.[16] In a 1D RPLC-MS separation of the same sample, only 1218 ion pairs were observed. A similar approach was recently published utilizing supercritical fluid chromatography (SFC) for fractionation of lipids by lipid class.[6,17] In this approach, 404 lipids were identified with the SFC fractionation workflow compared to 150 with a 1D RPLC-MS approach. Various column chemistry combinations have also been evaluated for orthogonality and application to compound identification.[18,19] Due to their orthogonality and suitability for both polar and apolar metabolites, RPLC × HILIC and ion exchange × RPLC configurations yielded the greatest identification performance for urine metabolites.[18] Taken together, these studies provide evidence for the potential of LC × LC to improve detection and identification of low-abundance metabolites. In our present work, we describe a strategy to harmonize a single high-resolution LC × LC-MS/MS analysis with data from typical-length 1D LC-MS runs, harnessing the benefits of LC × LC for compound identification while avoiding any significant decrease in throughput.

While human plasma and urine have been extensively evaluated using a multitude of techniques including a limited number of LC × LC methods,[11,20−23] the fecal metabolome remains substantially less well characterized, even as evidence gathers of the importance of the gut microbiome and its interaction with host metabolism.[24−29] In this study, we demonstrate an offline LC × LC-MS/MS metabolomics approach to identify low abundance human fecal metabolites in a small group of subjects that received a fecal microbiota transplant (FMT) for treatment of recurrent *Clostridioides difficile* (*C. diff*) infection (rCDI). Multiple criteria were used to assess accuracy and confidence of these compound identifications, including MS/MS database search score criteria, RT alignment with authentic standards, and comparison of experimental and computationally predicted RT. Compared with conventional (20 min) 1D separations, our offline two-dimensional methods (RPLC × HILIC and RPLC × RPLC) more than doubled the number of unique database match assignments (1513 to 3414) and identified 72 more metabolites that significantly differentiated pre- and post-FMT samples. The differential compounds include bile acids, amino acids, lipids, and several previously unreported metabolites. Our work complements a recent manuscript by Stewart et al.[29] that studied FMT samples from the same clinical trial, and includes data from four additional subjects. Furthermore, whereas Stewart et al. focused on targeted analysis of bile acid-related compounds using LC-IMS-MS, our method identified a broader range of metabolites using an untargeted workflow. Overall, our study demonstrates a practical, time-conscious strategy to enhance compound identification in metabolomics data using LC × LC-MS and applies this method to generate novel insight into the fecal metabolome in the context of FMT.

EXPERIMENTAL SECTION

Sample Collection and Extraction

All patients were enrolled under IRB #16−2283 at the University of North Carolina Hospital.[29] Fecal samples were collected pre-FMT and 2 weeks post-FMT for eight patients with prior unsuccessful antibiotic treatment for rCDI. Following collection, samples were stripped of all personally identifiable information and relabeled using the designations R3, R4, R7, R8, R9, R12, R13, and R14 for each of the 8 recipients included in the study, with the suffixes "-1" and "-2" appended to designate pre- and post-FMT samples, respectively. Samples were sent to the analysis laboratory on dry ice where they were stored at −80 °C. On the day of extraction, samples were weighed into pretared 2 mL screw-top polypropylene vials, and one 2.8 mm stainless steel bead was added to aid homogenization. Chilled extraction solvent was added to the tubes at a ratio of 5 mL solvent per 1 g feces and was comprised of 1:1:1 methanol:acetonitrile:acetone containing 10 mM of D_3-creatine, D_{10}-isoleucine, D_2-biotin, D_5-tryptophan, D_3-caffeine, D_3-octanoylcarnitine, D_3-palmitoylcarnitine, D_4-deoxycholic acid, D_4-cholic acid, and D_7-arginine as internal standards. Metabolites were extracted from the samples using a Precellys Evolution homogenizer (Bertin Corp., Montigny-le-Bretonneux, France) using two 20 s cycles at 6,200 rpm, separated by a 30 s break. Following extraction, samples were centrifuged for 10 min at 17,000 r.c.f. A 100 mL

https://doi.org/10.1021/acs.jproteome.4c00022
J. Proteome Res. 2024, 23, 2000−2012

aliquot of supernatant was transferred to clean microcentrifuge vials, dried under a gentle stream of nitrogen, and stored at −80 °C. On the day of analysis, the dried extracts were reconstituted as described below. Pooled samples were prepared by combining equal volumes of reconstituted fecal matter extract from all subjects.

First Dimension: Semipreparative LC with Fraction Collection

For pooled samples analyzed using offline LC × LC, semipreparative RPLC (SP-RPLC) of 2-fold concentrated fecal matter extract (1800 mL total dried extract reconstituted in 900 mL 9:1 water: methanol) was performed on a Waters (Milford, MA) Atlantis T3 OBD prep column (10 × 150 mm; 5 mm particle diameter) using an Agilent (Santa Clara, CA) 1200 liquid chromatograph equipped with a 900 μL injection kit. The column compartment was maintained at 55 °C. Mobile phase A was water with 0.1% v/v formic acid and mobile phase B was methanol with 0.025% v/v formic acid. The chromatographic gradient was as follows: 0−1 min 0% B; 1−20 min 100% B; 20−40 min 100% B. The flow rate was 3 mL/min and a postcolumn tee was used to establish a 50:1 effluent split between a Bio-Rad (Hercules, CA) BioFrac fraction collector and an Agilent 6520 quadrupole time-of-flight mass (QTOF) spectrometer operated as described in the Supporting Information. The resulting MS data was used for real-time monitoring of the semipreparative separation and initial screening of fraction contents, but not for compound identification or quantitation. Ninety-four 0.35 min fractions with a volume of 1.05 mL each were collected into tapered-base glass autosampler vials (Thermo Scientific) beginning at 3.0 min postinjection of the semipreparative method. The fractions were then dried using a GeneVacâ Ez-2 (Ipswich, United Kingdom) vacuum centrifuge at room temperature. The dried fractions were reconstituted in 50 mL of method-specific reconstitution solvent (85:15 acetonitrile:water for HILIC analysis or 9:1 water:methanol for RPLC analysis). Adjacent fractions were combined, resulting in forty-seven 100 mL fractions. Five mL of each fraction was analyzed by analytical LC-MS/MS as described below.

Second Dimension: Analytical LC-MS/MS

Fecal samples from individual human subjects, fractionated and unfractionated pooled samples, and authentic standards (which are listed in the Supporting Information) were analyzed by HILIC (Waters BEH Amide, 2.1 × 100 mm, 1.7 mm) and high-pH RPLC (Waters Charged-Surface Hybrid [CSH] C18, 2.1 × 100 mm, 1.7 mm) in both positive and negative ion modes on a Thermo Vanquish Horizon LC coupled to an Orbitrap ID-X mass spectrometer. For HILIC separations, mobile phase A consisted of 95:5 water:acetonitrile with 10 mM ammonium formate plus 0.125% v/v formic acid and mobile phase B was 5:95 water:acetonitrile with the same additive concentrations. HILIC separations utilized the following gradient: 0 min, 100% B; 0−0.5 min 100% B; 0.5−7 min 85% B; 7−9 min 85% B; 9−16 min 50% B; 16−16.1 min 100% B; 16.1−20 min 100% B. For RPLC separations, mobile phase A consisted of water with 10 mM ammonium acetate plus 0.025% ammonium hydroxide (v/v) and mobile phase B was methanol with the same additives. RPLC separations utilized the following gradient: 0 min 0% B, 0−5 min 60% B; 5−13 min 99% B; 13−17 min 99% B; 17−17.1 min 0% B; 17−20 min 0% B. A five μL injection volume was used for both separation modes. Data-dependent MS/MS was collected in positive and negative ion modes using parameters listed in the Supporting Information.

Data Processing and Compound Identification

MS^1 feature detection, integration, alignment, and adduct annotation was performed in Thermo Compound Discoverer 3.3 as described in the Supplemental Methods. Peak areas for the internal standards were assessed for reproducibility before and after normalization. Univariate and multivariate statistical analysis of the metabolomics data was performed following median normalization and log transformation using MetaboAnalyst 5.0.[30] To detect features that were differentially abundant between pre- and post- FMT sample groups, we used an unpaired students *t* test with Benjamini-Hochberg False Discovery Rate (FDR) correction for multiple comparisons. The threshold for statistical significance of differential features was assigned as a minimum of ±1.25-fold change with an FDR-corrected p-value of 0.1 or lower.

Compound identification using MS/MS data was performed using our software tool *MetIDTracker*, which has been described previously.[11] Both identity and "hybrid" spectral search were performed against public and commercially available libraries using the parameters described in the Supporting Information. To supplement spectral search scores, both an endogenous metabolite library of ∼1000 compounds and retention time prediction using the ReTip software package[31] were used to further qualify compound identifications; details regarding application of these methods are described in the Supporting Information. Metabolite identification confidence levels were assigned as follows. Only features satisfying MS/MS search score criteria (entropy score greater than or equal to 0.65) and with close RT alignment (±0.5 min) to the matching analytical standard were designated as MSI level 1 (MSI1) identifications.[32] Similarly, MS/MS library hits matching the structure of a compound in our library of authentic standards that did not align with the experimentally measured retention time were downgraded to compound class-level annotations (MSI3). Spectral hits to compounds for which we did not possess an authentic standard, but with a measured retention time within ±1.0 min of retention time predicted by Retip, were classified as MSI2A identifications. Features matched as identity hits by MS/MS entropy score alone were termed MSI2B identifications. All features assigned a MSI level of 1, 2A, or 2B are hereafter referred to as "identifications". Compound-class-level MSI3 annotations were assigned for features meeting one or more of the following criteria: NIST hybrid score[3] 600, 0.5 ≤ identity MS/MS entropy score <0.65, or in-source MS/MS entropy score[3] < 0.65.[33] Remaining detected features were classified as MSI4 (unknowns). MSI3 and MSI4 features were further consolidated to the highest intensity MS/MS feature within 0.2 min and ±0.0025 m/z. The number of identifications by each method was assessed by determining the number of compounds with a unique InChIKey (first 14 characters) with an MSI1, MSI2A, or MSI2B identification level. Compounds identified in four or more fractions were considered background ions and removed from the tally of unique compounds.

https://doi.org/10.1021/acs.jproteome.4c00022
J. Proteome Res. 2024, 23, 2000−2012

RESULTS AND DISCUSSION

Response of the Metabolome to Fecal Microbiota Transplantation

As reported previously, fecal microbiota transplant causes significant alteration to the fecal microbiome and metabolome.[34,35] To detect metabolites with differential abundance between pre- and post-FMT time points, samples from subjects with rCDI (8 pre-FMT samples and 8 post-FMT samples) were first analyzed by analytical RPLC- and HILIC-MS/MS as described above. Total ion chromatograms (TIC) of the fecal extracts under the different modes of chromatography and ionization are shown in Figure S1. High variability in the intersubject fecal metabolome is expected due to differences in diet, microbiome, and other factors.[36,37] One notable feature of the data was the presence of sizable clusters of peaks in the RPLC separation in the retention time range from 3 to 6 min (Figure S1A-B). These were attributed to polyethylene glycol (PEG) polymers, which were likely present due to pre-FMT bowel prep.[38,39] PEG-related ions were removed from the data before statistical comparison of pre- and post-FMT samples. However, ion suppression of metabolites eluting near PEG may have reduced the ability to accurately detect differential metabolites in this retention time range.[40]

While we have shown previously that preconcentration strategies are beneficial for compound identification,[11] routine metabolomics data collection and quantitation is achieved using conventional sample loading and typical run length (~20 min), thus all comparisons of pre- and post-FMT samples was performed using these methods. Principal component analysis (PCA) revealed a large separation between pre- and post-FMT samples in the first two principal components (Figure S2). A slight overlap of the 95% confidence intervals is seen for three of the four PCA plots; subject R3, which had particularly high levels of PEG, was consistently the furthest from the other samples within the group. The significantly up- and down-regulated features contributing to sample group differentiation are illustrated in volcano plots in Figure S3. In total, 2146 features were significantly differential between pre- and post-FMT sample groups; these features were later aligned to the MS/MS data for compound identification. A complete listing of differential features and all identified compounds are included in the Supporting Information (Metabolomics Workbench data upload).

Assigning Confidence to Metabolite Identifications

Several classification schemes have been proposed to report identification confidence for metabolomics data, however, assignment to a specific level in most schemes is subject to interpretation. For instance, using the original Metabolomics Standards Initiative ID levels an MSI2 identification is generally regarded as requiring a MS/MS spectral match, but no specific search algorithm, score threshold or confidence criteria are specified.[32,41,42] Higher confidence identifications can be achieved when multiple pieces of experimental evidence including retention time alignment with authentic standards is performed. However, purchasing and analyzing such libraries is costly, and no library covers all possible metabolites. To assess identification confidence to metabolites not included in our in-house authentic standard library, retention time prediction (RTP) for RPLC and HILIC models were created with the R package Retip.[31] Both experimentally measured retention times and the predicted RT models are in the Supporting Information (Metabolomics Workbench data upload). Replicate RTP model performance is reported in Tables S1−S2 and Figure S4. Modeling HILIC retention was less accurate than RPLC retention likely due to its more complex mechanism of separation.[43−45] It is our observation that RTP accuracy is not sufficient to confidently confirm identifications, but it adds supporting evidence if observed and predicted retention times align within an empirically determined margin, which was selected as ±1 min for this study.

In addition to RT prediction, searching MS/MS data against spectral libraries remains an essential component of compound identification in untargeted metabolomics. Spectral entropy scoring, an alternative to conventional dot-product algorithms, has recently been demonstrated to reduce false positive metabolite identification rates.[46] Entropy scores range from 0 to 1 with higher values generally representing more accurate matches. We observed that accurate metabolite identifications, supported by RT alignment to authentic standards or well-matched predicted RT, were often observed with entropy scores of 0.65 and above. We therefore selected this threshold as a reasonable balance between identification confidence and false discovery. An example head-to-tail plot of diltiazem, a common antihypertensive drug, is shown in Figure S5. This match had an entropy score of 0.681 and excellent retention time alignment to a pure standard. The combination of entropy score and RT prediction (or RT matching when authentic standards were available) were used to assign metabolite ID confidence levels for all reported features.

Assessing Identification Performance of 1D- and 2D-LC Approaches

To rigorously evaluate the potential of offline 2D separations to improve compound identification performance and to assess whether the increased time and sample consumption they require is justified, 2D methods must be assessed relative to typical 1D separations. Prior to MS/MS data collection, an exclusion list of background ions was created by running a RPLC and HILIC blank injection of the corresponding reconstitution solvents. Then five iterative LC-MS/MS runs of a pooled fecal sample were performed with run-to-run precursor ion exclusion enabled.[47] Compounds were identified in the resulting data according to criteria described in the methods and were tabulated (Figure S6). The number of unique identifications increased with each successive injection but trended toward a plateau for both ionization modes and separations. 931 and 288 total identifications (MSI1, MSI2A and MSI2B) were observed for the RPLC separations in positive and negative mode, and 545 and 292 were observed using HILIC. Lower identification totals for negative mode were expected, as the acidity of the mobile phases favored the formation of positive ions. This compromise was accepted to allow retention time alignment between ionization modes. 1147 unique identifications were made by RPLC and 770 by HILIC when positive and negative mode results were combined; 1513 unique identifications were made in total for all 1D methods. MSI-level feature breakdowns for each 1D method are illustrated in Figure S7. Greater than 65% of collected MS/MS features for all methods were classified as unknowns.

A semipreparative RPLC (SP-RPLC) first dimension separation at low pH performed on a 10 mm inner diameter Waters High Strength Silica T3 column was used as the first dimension for all 2D analyses. Semipreparative HILIC was also

https://doi.org/10.1021/acs.jproteome.4c00022
J. Proteome Res. 2024, 23, 2000−2012

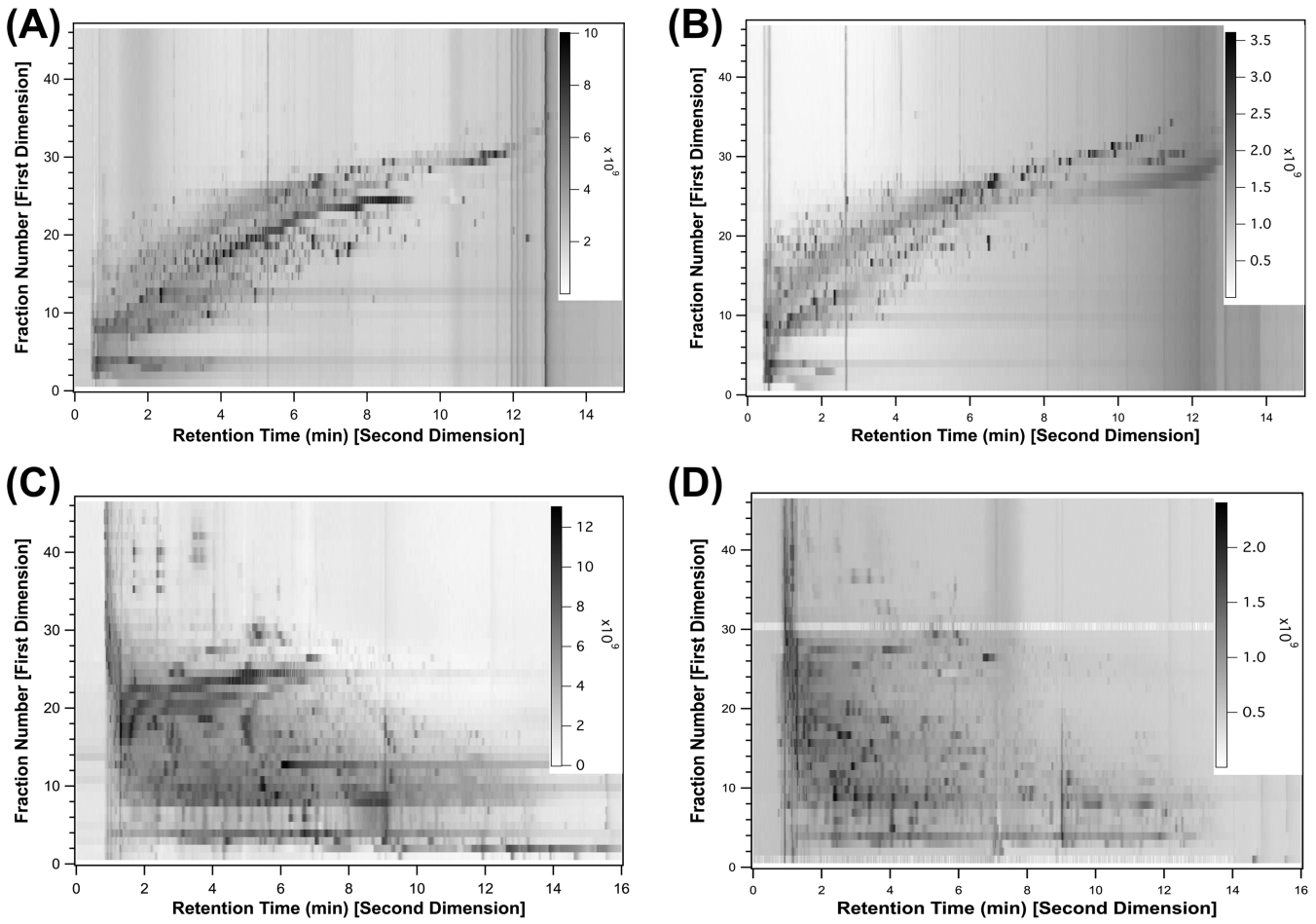

Figure 1. Two-dimensional TICs derived from LC-MS analysis of fractionated pooled fecal extract using (A) SP-RPLC positive mode, (B) SP-RPLC negative mode, (C) SP-HILIC positive mode, and (D) SP-HILIC negative mode methods. The logarithm of TIC intensity is represented by grayscale.

evaluated as a first dimension, but it was determined to have lower loading capacity than RPLC, making it difficult to prepare high-concentration fractions for subsequent analysis. A preparative-scale HILIC column or pooling fractions from multiple runs could be used to increase loading capacity, but would have required either different instrumentation or more time for fraction collection and drying, and was therefore not pursued further.[48]

The effective peak capacity of offline 2D separations is determined by several factors, including the peak capacity of each separation, separation method orthogonality, and fraction sampling frequency.[49,50] We evaluated LC × LC performance for metabolite identification using two different second-dimension columns. First, a high-pH RPLC separation (Waters Charged Surface Hybrid column) was used to improve orthogonality with the low-pH first dimension separation. Our second method, HILIC (Waters BEH Amide column), is inherently more orthogonal to RPLC, thus we expected a higher total peak capacity using this approach. Several previous studies have systematically investigated column combinations and orthogonality in greater detail;[18,19] our study focuses on the potential for enhanced metabolite identification and compound classification using SP-LC × LC-MS.

A TIC from the first dimension SP-RPLC separation is shown in Figure S8. The TICs for the full LC × LC separations are illustrated as heatmaps with peak intensity visualized as a logarithmically scaled grayscale gradient in Figure 1. A clear diagonal band of peaks can be seen for the SP-RPLC × RPLC separation in which high-pH RPLC was used as the second dimension, revealing limited orthogonality with the first-dimension separation. For the SP-RPLC × HILIC separation, compounds that eluted earlier from the first dimension (polar compounds) were spread over a wider range of the second dimension (HILIC) separation space, whereas late-eluting nonpolar compounds were lightly retained and eluted early in the HILIC gradient. The number of unique identifications made per fraction (Figure S9) further illustrates the difference in orthogonality between the methods, as more identifications in the first ∼20 fractions were observed with SP-RPLC × HILIC. In total, 1479, 555, 1917, and 830 identifications were made when RPLC positive mode, RPLC negative mode, HILIC positive mode, and HILIC negative mode were used as the second-dimension method, respectively. 1917 and 2548 unique identifications were made in total for both modes of the RPLC and HILIC methods, and 3414 total unique identifications were achieved across all 2D methods. Figure 2 summarizes the total number of identifications made by each of the 1D and 2D methods.

Compared to 1D separations, 2.25 times as many metabolites were identified by the offline 2D approaches, and a much higher number of MS/MS features were detected with a comparable proportion of unknowns (Figure S10).

https://doi.org/10.1021/acs.jproteome.4c00022
J. Proteome Res. 2024, 23, 2000−2012

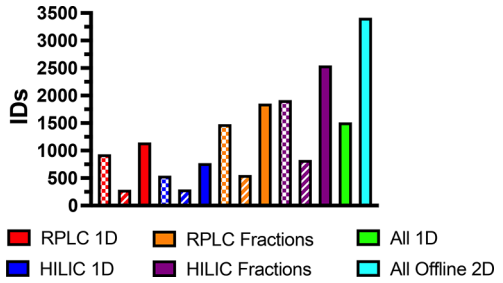

Figure 2. Total number of unique identified compounds (MSI1, MSI2A, and MSI2B) observed by each method. Checkered and striped fill patterns are for positive and negative mode methods, respectively. Solid bars are a combination of both ion modes. "All 1D" encompasses the total number of unique identifications made by "RPLC 1D" and "HILIC 1D" methods in, while "All Offline 2D" includes the total number of unique identifications made by "RPLC Fractions" and "HILIC Fractions."

Compared to 1D methods, a slightly larger proportion of the identifications achieved with the offline 2D methods were classified as MSI1 (11.5% versus 10.8%) and MSI2A (59.7% versus 46.8%) confidence levels. We have observed previously that the use of multirun precursor ion exclusion and high sample loading as strategies for increasing the number of compounds identified also tends to yield a higher total number and higher proportion of unidentified (MSI4) features.[11] In this study, however, the offline 2D methods identified a comparable proportion of the unknown MS/MS features to our standard 1D method. This suggests that breaking a complex sample into simpler fractions may generate cleaner MS/MS spectra that are more amenable to identification by library searching. Supporting this hypothesis, average precursor ion purity, a metric of how many different ions exist within the quadrupole isolation window of the MS scan, was modestly (~5−10%) but consistently lower (i.e., less "pure") for 1D than 2D separations and had a broader distribution for all identification levels (Figure S11). As precursor ion purity decreased, so did identification confidence; higher proportions of MSI4 features for 1D methods may also partly explain this observation. Additional factors underlying the increased number of identified compounds observed using LC × LC may include reduction in ionization suppression in the fractionated samples, improved MS/MS coverage of low abundance precursors, and the ability to load higher concentrations of a limited number of metabolites in each fraction without overloading the column as would likely occur if the mass loading of an unfractionated sample were significantly increased.

Iterative LC-MS/MS acquisition of the fractions was not performed to keep instrument run time under ~16 h for each separation and ionization mode combination. However, the potential benefit of using iterative MS/MS for deeper annotation of individual fractions was investigated using several fractions of varying abundance and regions of the first-dimension chromatogram (Figure S12). With each iterative injection, more metabolites were identified in each fraction, suggesting that further gains in compound identification could be achieved by combining fractionation with iterative LC-MS/MS runs of each fraction, if sample and runtime are not limited. Nevertheless, even the first injection of an iterative LC-MS/MS sequence resulted in the identification of more compounds than were observed in a typical single-injection, noniterative data-dependent acquisition LC-MS/MS worklist.

Many metabolites were identified by both 1D and 2D approaches, but 2261 metabolites were identified only using the offline LC × LC methods (see UpSet plot in Figure S13). A much smaller number of metabolites, 360, were only identified using 1D methods. These limited losses may be attributed to the additional sample manipulation required for 2D approaches (drying/reconstitution), slightly different thresholds for removal of high-scoring database matches by iterative methods (creation of an exclusion list), and exclusion of metabolites found in more than four fractions. Thus, to maximize total compound identification, it is still worthwhile to acquire LC-MS/MS data using an unfractionated sample in addition to performing separate analyses of each fraction.

Evaluating Coverage of the Fecal Metabolome

Compound class information for all unique metabolite identifications and MSI3 annotations from a pooled fecal extract is shown in Figure 3. The most common chemical

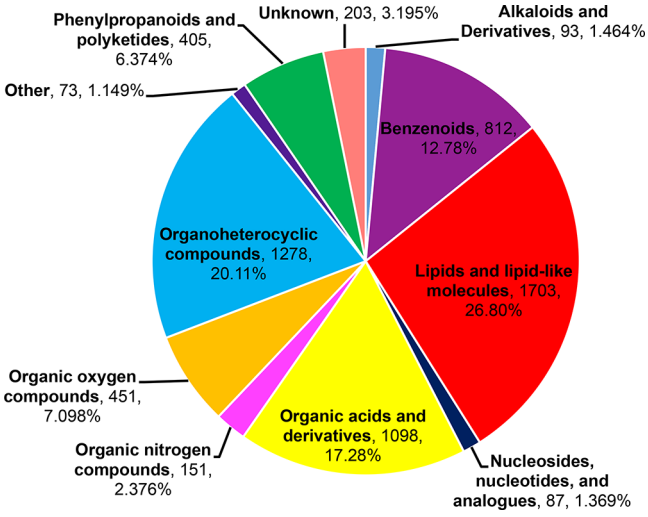

Figure 3. Compound class breakdown of all unique InChIKeys assigned an MSI1, MSI2A, MSI2B, and MSI3 identification level.

classes observed (by superclass level according to ClassyFire ontology)[51] were lipid and lipid-like molecules (26.80%), organoheterocyclic compounds (20.11%), and organic acids and derivatives (17.28%). Certain subclasses of particular relevance to the fecal metabolome, including bile acids and fatty acid esters, were prevalent in this sample; these observations are discussed in more detail in the next section. While "lipid and lipid-like molecules" was the most common superclass observed, it exhibited the lowest improvement in the number of unique identifications and compound class annotations achieved with offline 2D approaches (Figure S14). The greatest improvement in unique compound class annotations with fractionation and preconcentration was for benzenoids and nucleosides/nucleotides, which both demonstrated over a 3-fold increase from 1D methods. A substantial proportion (>65%) of features in the data set remained unidentified. While some of these unknown features represent degenerate fragment ions, adducts, and contaminants, another portion likely represent previously unannotated or unreported fecal metabolites. Strategies for the identification of such unknowns are discussed below.

https://doi.org/10.1021/acs.jproteome.4c00022
J. Proteome Res. 2024, 23, 2000−2012

Several recent studies have explored the fecal and lumen metabolomes, seeking improved understanding of the biology of this previously poorly characterized compartment of human and mammalian physiology. In one study, a small diameter tube that was advanced from the stomach and duodenum to the jejunum was used to collect samples from the human gut for 8.5 h.[28] Eight hundred twenty-eight unique metabolites, including bile, food, and protein breakdown metabolites, were identified from a single healthy human participant consuming food and water *ad libitum*.[28] In a recent set of companion publications, noninvasive robotic sampling capsules with pH-sensitive coatings were ingested by a cohort of 15 human participants. This allowed for sampling different regions in the small intestine.[26,27] A total of 1909 metabolites were identified; several significant clusters related to fruit, alcohol, dessert, and caffeine consumption were also annotated.[26] A recent study on a larger cohort of subjects focused on the repeatability and reproducibility of detection and quantitation of targeted metabolites in feces using multiple extraction protocols.[52] A total of 360 metabolites and 132 lipids detected by LC-MS/MS were reported in these fecal extracts LC-MS. A study of antibiotic-induced shifts in the mouse gut microbiome and metabolome identified 480 metabolites in the mouse cecum.[53] Secondary bile acids, glucose, free fatty acids, and dipeptides notably decreased, while primary bile acids and sugar alcohols increased with antibiotic treatment which allowed for colonization of *C. diff*. Of the 3774 unique metabolites we matched to a MS/MS database, at least 793 were also identified in one or more of the studies cited above. Different sample types, participants, and our distinct analytical methods likely resulted in many of our identified compounds not having been reported elsewhere. Among the compounds observed uniquely in our study, 49 and 2217 metabolites were classified at MSI confidence levels 1 and 2A, respectively.

Merging Identifications and Significantly Differential Features from FMT

Compared to 1D methods, 2D approaches identified on average 1.6 times more features that were significantly differential between pre- and post-FMT samples (Table 1). Identifying more relevant features by 2D approaches produced a clearer picture of metabolic changes associated with receiving an FMT, including biological insights regarding the response of the fecal metabolome to FMT to treat rCDI. Prior to *C. diff* infection, dysregulation of bile acids, amino acids, fatty acid esters, and carbohydrates have been reported previously as signals of alterations in microbial metabolism.[54−60] Our data provides additional detail regarding the impact of FMT on these metabolite classes. Volcano plots for the corresponding ClassyFire subclasses are shown in Figure 4. Our results confirmed previous trends that primary bile acids (i.e., glycocholic acid and taurocholic acid) decreased, and secondary bile acids (i.e., taurodeoxycholic acid, lithocholic acid, deoxycholic acid) increased following FMT (Figure 4A), reflecting recolonization of the gut with active microbiota.[29,54,61,62] N-acetylated amino acids (Figure 4B) have been reported to decrease with *C. diff* colonization;[63] N-acetylarginine, N-acetyllysine, N-acetylvaline, N-acetylthreonine, and N-acetylglutamic acid were found to increase significantly following FMT. Prolylhydroxyproline, an amino acid that is beneficial for *C. diff* growth, and released during toxin-mediated CDI from host collagen,[62−65] was also found to decrease substantially following FMT. Carbohydrates (Figure 4C), including sorbitol, melezitose, and maltose, have been identified as significant carbon sources for *C. diff* growth; we observed a decrease in abundance of these compounds following FMT.[54,63] FMT also affected carnitine metabolism (Figure 4D). Intracellular shifts in carnitine concentration in bacteria have been observed and attributed to a cellular response to osmotic stresses.[66] Interpretation of the biological significance of these observations and identification of unknown fecal metabolites is complex due to intermixing of human and microbial metabolism. Both represent major topics of ongoing research in our laboratories.

Table 1. Alignment of Significant FMT-Related Features to MS/MS Data and the Number of Unique IDs by Each Method

Method	Found lookup features	Missed lookup features	Unique IDs
RPLC 1d Pos	330	96	75
RPLC Fractions Pos	340	86	97
RPLC 1d Neg	452	68	52
RPLC Fractions Neg	311	209	83
HILIC 1d Pos	363	179	88
HILIC Fractions Pos	481	61	158
HILIC 1d Neg	468	190	63
HILIC Fractions Neg	459	199	103

Identification of Recently Discovered and Novel Metabolites

Use of LC × LC-MS/MS improved the signal and spectral quality of many unknown features compared to conventional 1D LC-MS/MS for a pooled fecal extract. However, the resulting higher quality MS/MS data did not always result in matches when searched against our set of spectral libraries. Such libraries continue to expand but remain incomplete and may be deficient in compounds related to bacterial metabolism which are abundant in the fecal metabolome. Continued improvements with *in silico* based structure prediction methods, including those implemented by software tools like SIRIUS, CANOPUS, and COSMIC, may help prioritize and identify unknown features.[67−69] We assessed the subset of unknown metabolites that were significantly different between pre- and post FMT samples using each of these tools. SIRIUS proposed 7-oxoglycodeoxycholic acid as a probable identification (0.865 COSMIC score) of a previously unidentified feature (Figure 5). An MS/MS spectrum of 7-oxoglycodeoxycholic acid did not exist in any of the reference libraries searched. To date, no other studies in Metabolomics Workbench have reported this compound as an identified metabolite, although other literature sources have suggested it as a plausible secondary bile acid that could be generated by bacterial metabolism.[70]

A specific focus on annotating microbially conjugated bile acids (MCBAs), bile acids conjugated with other amino acids than glycine- and taurine, was motivated by recent research that proved the existence of multiple such novel conjugated bile acids.[26,29,71] In the context of *C. diff* infection, bile salt hydrolases have been reported to alter the pool of MCBAs present and to potentially alter virulence of the infection.[72] MCBAs were first identified in samples collected from the small intestine and are expected to have higher concentration

https://doi.org/10.1021/acs.jproteome.4c00022
J. Proteome Res. 2024, 23, 2000−2012

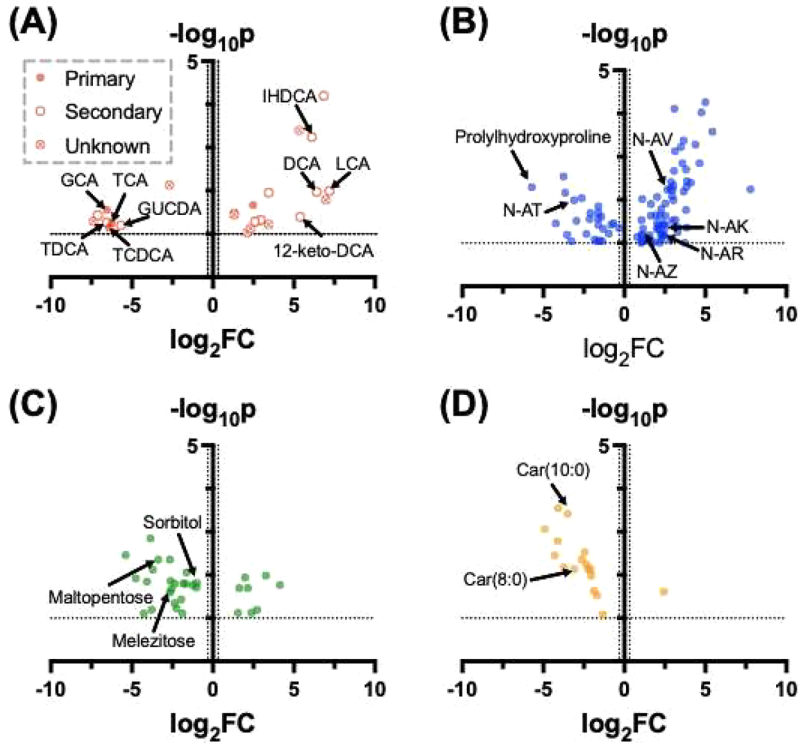

Figure 4. Volcano plots of unique significant MSI level 1−3 (A) bile acids, alcohols, and derivatives, (B) amino acids, peptides, and analogs, (C) carbohydrates and carbohydrate conjugates, and (D) carnitines. MS/MS features corresponding to the same compound were consolidated to the highest confidence and highest intensity feature observed in any experiment. Fold change is reported as the difference between post-FMT to pre-FMT samples. Specific bile acids glycocholic acid (GCA), taurocholic acid (TCA), glycoursodeoxycholic acid (GUCDA), taurodeoxycholic acid (TDCA), taurochenodeoxycholic acid (TCDCA), isohyodeoxycholic acid (IHDCA), deoxycholic acid (DCA), lithocholic acid (LCA), and 12-ketodeoxycholic acid (12-keto-DCA) are highlighted. N-acetylated amino acids shown are simplified to "N-A" followed by the single letter code for the corresponding amino acid. Sorbitol, maltopentose, and melezitose were all downregulated. Carnitine (Car) 8:0 and 10:0 were also downregulated.

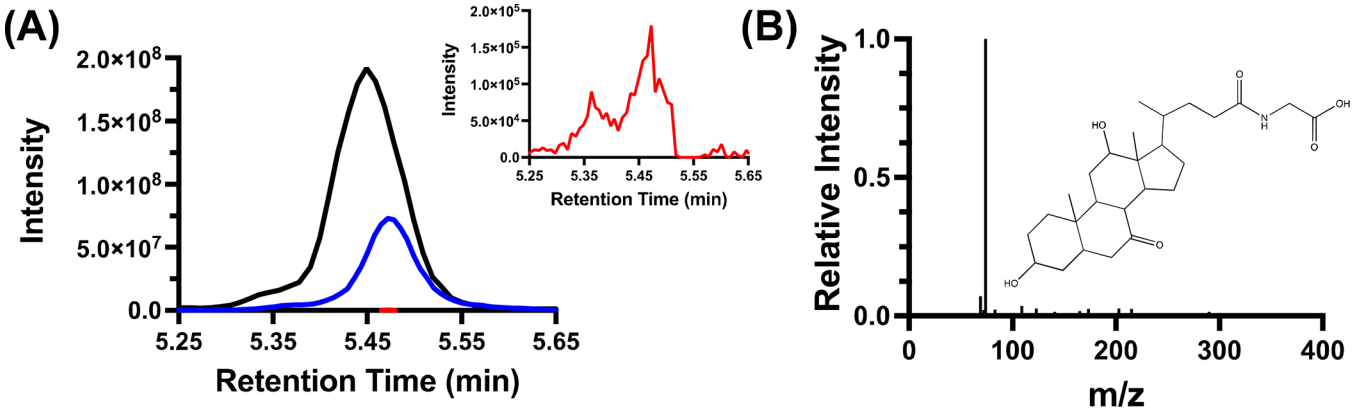

Figure 5. Unidentified differential feature (pre vs post-FMT) detected using HILIC negative ion mode. (A) extracted ion chromatograms of 426.2861 *m*/*z* from 1D separations of a (blue) pre-FMT pool and (red) post-FMT pool compared to (black) fraction 25. (B) Experimental MS/MS and proposed identification 7-oxoglycodeoxycholic acid.

in that location within the gut. Furthermore, MCBAs are relatively low-abundance compounds, reported as generating approximately three times lower signal than canonical bile acids in human fecal extracts.[29] Nevertheless, we confirmed the identification of 16 of the 22 MCBAs reported by Shalon et. al in human fecal samples using offline 2D HILIC by precursor *m*/*z* and alignment of two expected fragment ions (see Supporting Information).[26] An extracted ion chromatogram and MS/MS spectrum for once MCBA, tyrosocholic acid, is shown in Figure S15. Five other MCBAs could be matched by precursor mass with reasonable chromatographic peaks but lacked confirmatory MS/MS evidence in our data, whereas only Cys-trihydroxlated bile acid was not detected. Notably, none of the MCBAs identified were found to differ significantly between pre- and post-FMT samples, although targeted methods with lower detection limits would allow more accurate quantitation and differential analysis of these low-abundance compounds.

As an additional approach to categorize unknown features in our fecal samples, we employed spectral networking analysis

https://doi.org/10.1021/acs.jproteome.4c00022
J. Proteome Res. 2024, 23, 2000−2012

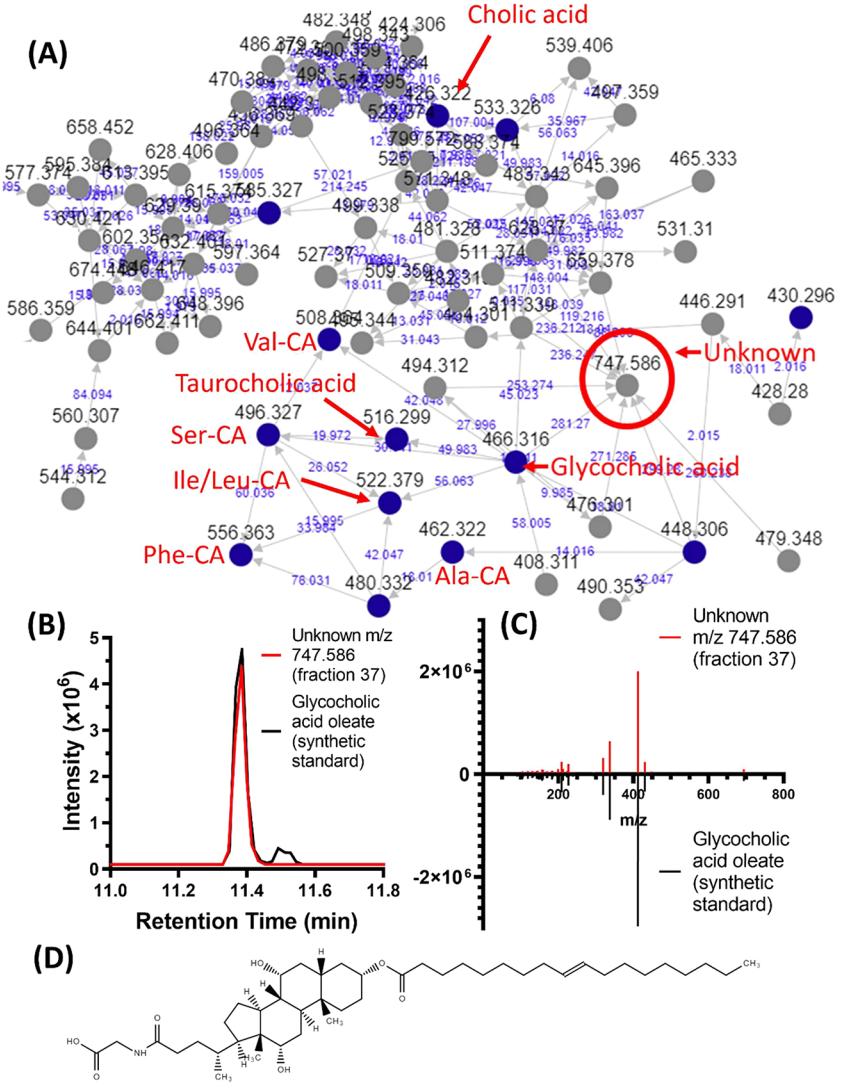

Figure 6. (A) GNPS network containing bile acids and related unknowns. (B) Overlaid chromatographic trace and (C) head-to-tail MS/MS spectrum of unknown feature with *m/z* 747.586 and synthesized GCA-oleate. (D) proposed structure of GCA-oleate.

using the Global Natural Products Social Molecular Networking tool (GNPS, https://gnps.ucsd.edu) as described in Supporting Information.[73] One resulting subnetwork, illustrated in Figure 6A, contained an unknown compound with *m/z* 747.586 that was closely associated with the spectrum of glycocholic acid, but it was observed at a distinct HILIC retention time in a later RPLC chromatographic fraction. Noting the mass difference of 281.27 Da between the unknown and glycocholic acid, we speculated the compound could be an fatty acid esterified bile acid (FA-BA), a compound class which has been hypothesized based on classical assay methods[74,75] and has only recently begun to be characterized by LC-MS/MS.[76] We synthesized an oleate ester of glycocholic acid and several other bile acids and used this to confirm the identity of the unknown feature as an $[M+NH_4]^+$ adduct of glycocholic acid oleate (Figure 6B-D), which to our knowledge has not been reported previously. Further examination of our LC × LC-MS/MS data revealed the presence of at least 13 additional fatty acid esterified bile acids (FA-BA) (Table S3). FA-BA are believed to originate from bacterial metabolism and may play a role in modulating host immunity or in reducing the effective concentration of specific cytotoxic bile acid species.[76]

For remaining unknown features for which current *in silico* and data searching strategies yield no results, collecting nuclear magnetic resonance (NMR) data may be possible with our 2D approach, especially if the second-dimension separation were scaled up to match the semipreparative first dimension. Low mM concentrations are typically required for ^{1}H NMR identification of unknown compounds, but improvement in instrument sensitivity has yielded promising results for lipid identification using analytical-scale LC-MS.[77] Preconcentration of semipreparative fractions may allow even moderate abundance metabolites to produce sufficient NMR signal for structural elucidation.

CONCLUSION

Our offline LC × LC-MS/MS method improved the number of unique features identified in a pooled human fecal extract by 2.25-fold compared to a typical strategy using iterative 1D LC-MS/MS. This result suggests the utility of high-resolution separations, including multidimensional separations, as a strategy to improve spectral matches and use in-silico structure prediction tools to identify unknowns in MS/MS data. Automated retention time alignment allowed us to perform

https://doi.org/10.1021/acs.jproteome.4c00022
J. Proteome Res. 2024, 23, 2000−2012

comprehensive LC × LC analysis on only a single pooled sample and permitted use of faster LC-MS runs on the remainder of the study samples, resulting in minimal impact on overall throughput. Using this approach, we identified significant differences in the fecal metabolome associated with FMT for recurrent *C. diff* infection, including both previously observed and novel alterations in bile acids, amino acids, carbohydrates, acylcarnitines, and multiple unknown compounds. Our study adds to the growing body of literature focused on understanding the depth of the human microbial metabolome and its connection with specific disease states such as *C. diff* infection, recurrence, and treatment. Many fecal metabolites and their potential interactions with their host organism remain as-yet unexplored. Ongoing efforts to deepen knowledge of the fecal microbiome and its metabolism, which may be facilitated by the approaches described here, can be expected to yield important insights relevant to human health and treatment of disease.

■ ASSOCIATED CONTENT

Data Availability Statement

All raw data files, a full list of authentic standards used in the study and their retention times, and additional related data files are available on the Metabolomics Workbench (https://www.metabolomicsworkbench.org), study ID ST002977.

Supporting Information

The Supporting Information is available free of charge at https://pubs.acs.org/doi/10.1021/acs.jproteome.4c00022.

Supplemental Methods, including materials and reagents, MS data collection parameters, data analysis parameters for software tools, and synthesis methods; Figure S1, total ion chromatograms preand post-FMT; Figure S2, principal component analysis pre- and post-FMT; Figure S3, volcano plots of differential features pre vs post FMT; Table S1, retention time prediction models for the RPLC; Table S2, retention time prediction models for HILIC; Figure S4, observed versus model-predicted RTs; Figure S5, head-to-tail MS/MS and extracted ion chromatogram of diltiazem; Figure S6, cumulative unique identifications made using iterative LC-MS/MS; Figure S7, MSI level feature consolidation chart; Figure S8, total ion chromatogram for semipreparative LC; Figure S9, compounds identified per fraction for 2nd dimension methods; Figure S10, MSI level feature distribution by fractions; Figure S11, precursor ion purity by MSI level for pooled fecal extract and fractions thereof; Figure S12, cumulative identifications for iterative LC-MS/MS of select fractions (PDF)

■ AUTHOR INFORMATION

Corresponding Author

Charles R. Evans − *Michigan Compound Identification Development Core, Biomedical Research Core Facilities, and Department of Internal Medicine, University of Michigan, Ann Arbor, Michigan 48109, United States;* orcid.org/0000-0001-6698-5330; Email: chevans@umich.edu

Authors

Brady G. Anderson − *Department of Chemistry and Michigan Compound Identification Development Core, University of Michigan, Ann Arbor, Michigan 48109, United States;* orcid.org/0000-0002-1239-3812

Alexander Raskind − *Michigan Compound Identification Development Core and Biomedical Research Core Facilities, University of Michigan, Ann Arbor, Michigan 48109, United States*

Rylan Hissong − *Michigan Compound Identification Development Core and Biomedical Research Core Facilities, University of Michigan, Ann Arbor, Michigan 48109, United States*

Michael K. Dougherty − *Department of Medicine, Division of Gastroenterology and Hepatology, University of North Carolina at Chapel Hill, Chapel Hill, North Carolina 27599, United States*

Sarah K. McGill − *Department of Medicine, Division of Gastroenterology and Hepatology, University of North Carolina at Chapel Hill, Chapel Hill, North Carolina 27599, United States*

Ajay S. Gulati − *Department of Medicine, Division of Gastroenterology and Hepatology, University of North Carolina at Chapel Hill, Chapel Hill, North Carolina 27599, United States; Department of Pathology and Laboratory Medicine, University of North Carolina at Chapel Hill, Chapel Hill, North Carolina 27599, United States*

Casey M. Theriot − *Department of Population Health and Pathobiology, College of Veterinary Medicine, North Carolina State University, Raleigh, North Carolina 27606, United States*

Robert T. Kennedy − *Department of Chemistry, Michigan Compound Identification Development Core, and Department of Pharmacology, University of Michigan, Ann Arbor, Michigan 48109, United States;* orcid.org/0000-0003-2447-7471

Complete contact information is available at: https://pubs.acs.org/10.1021/acs.jproteome.4c00022

Author Contributions

B.G.A, C.M.T., R.T.K., and C.R.E. designed the study. Data processing and compound annotation were performed by B.G.A and C.R.E.; R.H. prepared and annotated retention times of the MetaSci standards library. A.R. developed *MetIDTracker* software used for database searching and data alignment. Fecal samples from human subjects were collected under supervision of M.K.D., S.K.M., and A.G. Sample preparation and the collection of LC-MS experimental data were performed by B.G.A. and C.R.E. Analysis of statistically relevant features associated with FMT was performed by C.M.T., B.G.A., and C.R.E. All authors contributed to the writing and editing of the manuscript.

Notes

The authors declare no competing financial interest.

■ ACKNOWLEDGMENTS

This work was supported by the National Institutes of Health (NIH) Common Fund Metabolomics program, grant U2CES030164 to C.R.E. and NIH P41-GM108538 and NSF CHE-1904146 to R.T.K. The FMT study was supported by the NCTraCS Translational and Clinical Sciences Institute Pilot Grant UNCSUR11609.

REFERENCES

(1) Kuhl, C.; Tautenhahn, R.; Böttcher, C.; Larson, T. R.; Neumann, S. CAMERA: An Integrated Strategy for Compound Spectra Extraction and Annotation of Liquid Chromatography/Mass Spectrometry Data Sets. *Anal. Chem.* **2012**, *84* (1), 283−289.

(2) Kachman, M.; Habra, H.; Duren, W.; Wigginton, J.; Sajjakulnukit, P.; Michailidis, G.; Burant, C.; Karnovsky, A. Deep Annotation of Untargeted LC-MS Metabolomics Data with Binner. *Bioinformatics* **2020**, *36* (6), 1801−1806.

(3) Mahieu, N. G.; Huang, X.; Chen, Y.-J.; Patti, G. J. Credentialing Features: A Platform to Benchmark and Optimize Untargeted Metabolomic Methods. *Anal. Chem.* **2014**, *86* (19), 9583−9589.

(4) Mahieu, N. G.; Patti, G. J. Systems-Level Annotation of a Metabolomics Data Set Reduces 25 000 Features to Fewer than 1000 Unique Metabolites. *Anal. Chem.* **2017**, *89* (19), 10397−10406.

(5) Kind, T.; Tsugawa, H.; Cajka, T.; Ma, Y.; Lai, Z.; Mehta, S. S.; Wohlgemuth, G.; Barupal, D. K.; Showalter, M. R.; Arita, M.; Fiehn, O. Identification of Small Molecules Using Accurate Mass MS/MS Search. *Mass Spectrom. Rev.* **2018**, *37* (4), 513−532.

(6) Lu, W.; Su, X.; Klein, M. S.; Lewis, I. A.; Fiehn, O.; Rabinowitz, J. D. Metabolite Measurement: Pitfalls to Avoid and Practices to Follow. *Annu. Rev. Biochem.* **2017**, *86* (1), 277−304.

(7) Blaženović, I.; Kind, T.; Ji, J.; Fiehn, O. Software Tools and Approaches for Compound Identification of LC-MS/MS Data in Metabolomics. *Metabolites* **2018**, *8* (2), 31.

(8) Hu, Y.; Cai, B.; Huan, T. Enhancing Metabolome Coverage in Data-Dependent LC-MS/MS Analysis through an Integrated Feature Extraction Strategy. *Anal. Chem.* **2019**, *91*, 14433−14441.

(9) Rainey, M. A.; Watson, C. A.; Asef, C. K.; Foster, M. R.; Baker, E. S.; Fernández, F. M. CCS Predictor 2.0: An Open-Source Jupyter Notebook Tool for Filtering Out False Positives in Metabolomics. *Anal. Chem.* **2022**, *94* (50), 17456−17466.

(10) Asef, C. K.; Rainey, M. A.; Garcia, B. M.; Gouveia, G. J.; Shaver, A. O.; Leach, F. E.; Morse, A. M.; Edison, A. S.; McIntyre, L. M.; Fernández, F. M. Unknown Metabolite Identification Using Machine Learning Collision Cross-Section Prediction and Tandem Mass Spectrometry. *Anal. Chem.* **2022**, *21*, 55.

(11) Anderson, B. G.; Raskind, A.; Habra, H.; Kennedy, R. T.; Evans, C. R. Modifying Chromatography Conditions for Improved Unknown Feature Identification in Untargeted Metabolomics. *Anal. Chem.* **2021**, *93* (48), 15840−15849.

(12) Habra, H.; Kachman, M.; Bullock, K.; Clish, C.; Evans, C. R.; Karnovsky, A. MetabCombiner: Paired Untargeted LC-HRMS Metabolomics Feature Matching and Concatenation of Disparately Acquired Data Sets. *Anal. Chem.* **2021**, *93* (12), 5028−5036.

(13) Urban, P. L. Clarifying Misconceptions about Mass and Concentration Sensitivity. *J. Chem. Educ.* **2016**, *93* (6), 984−987.

(14) Bruins, A. P. Mechanistic Aspects of Electrospray Ionization. *J. Chromatogr. A* **1998**, *794* (1−2), 345−357.

(15) Sorensen, M. J.; Miller, K. E.; Jorgenson, J. W.; Kennedy, R. T. Two-Dimensional Liquid Chromatography-Mass Spectrometry for Lipidomics Using off-Line Coupling of Hydrophilic Interaction Liquid Chromatography with 50 Cm Long Reversed Phase Capillary Columns. *J. Chromatogr. A* **2023**, *1687*, No. 463707.

(16) Guo, K.; Peng, J.; Zhou, R.; Li, L. Ion-Pairing Reversed-Phase Liquid Chromatography Fractionation in Combination with Isotope Labeling Reversed-Phase Liquid Chromatography−Mass Spectrometry for Comprehensive Metabolome Profiling. *J. Chromatogr. A* **2011**, *1218* (23), 3689−3694.

(17) Berger, T. A. Separation of Polar Solutes by Packed Column Supercritical Fluid Chromatography. *J. Chromatogr. A* **1997**, *785* (1−2), 3−33.

(18) Grübner, M.; Dunkel, A.; Steiner, F.; Hofmann, T. Systematic Evaluation of Liquid Chromatography (LC) Column Combinations for Application in Two-Dimensional LC Metabolomic Studies. *Anal. Chem.* **2021**, *93* (37), 12565−12573.

(19) Yeung, D.; Mizero, B.; Gussakovsky, D.; Klaassen, N.; Lao, Y.; Spicer, V.; Krokhin, O. V. Separation Orthogonality in Liquid Chromatography-Mass Spectrometry for Proteomic Applications: Comparison of 16 Different Two-Dimensional Combinations. *Anal. Chem.* **2020**, *92* (5), 3904−3912.

(20) Bouatra, S.; Aziat, F.; Mandal, R.; Guo, A. C.; Wilson, M. R.; Knox, C.; Bjorndahl, T. C.; Krishnamurthy, R.; Saleem, F.; Liu, P.; Dame, Z. T.; Poelzer, J.; Huynh, J.; Yallou, F. S.; Psychogios, N.; Dong, E.; Bogumil, R.; Roehring, C.; Wishart, D. S. The Human Urine Metabolome. *PLoS One* **2013**, *8* (9), No. e73076.

(21) Blaženović, I.; Kind, T.; Sa, M. R.; Ji, J.; Vaniya, A.; Wancewicz, B.; Roberts, B. S.; Torbašinović, H.; Lee, T.; Mehta, S. S.; Showalter, M. R.; Song, H.; Kwok, J.; Jahn, D.; Kim, J.; Fiehn, O. Structure Annotation of All Mass Spectra in Untargeted Metabolomics. *Anal. Chem.* **2019**, *91* (3), 2155−2162.

(22) Simón-Manso, Y.; Lowenthal, M. S.; Kilpatrick, L. E.; Sampson, M. L.; Telu, K. H.; Rudnick, P. A.; Mallard, W. G.; Bearden, D. W.; Schock, T. B.; Tchekhovskoi, D. V.; Blonder, N.; Yan, X.; Liang, Y.; Zheng, Y.; Wallace, W. E.; Neta, P.; Phinney, K. W.; Remaley, A. T.; Stein, S. E. Metabolite Profiling of a NIST Standard Reference Material for Human Plasma (SRM 1950): GC-MS, LC-MS, NMR, and Clinical Laboratory Analyses, Libraries, and Web-Based Resources. *Anal. Chem.* **2013**, *85* (24), 11725−11731.

(23) Lawton, K. A.; Berger, A.; Mitchell, M.; Milgram, K. E.; Evans, A. M.; Guo, L.; Hanson, R. W.; Kalhan, S. C.; Ryals, J. A.; Milburn, M. V. Analysis of the Adult Human Plasma Metabolome. *Pharmacogenomics* **2008**, *9* (4), 383−397.

(24) Zierer, J.; Jackson, M. A.; Kastenmüller, G.; Mangino, M.; Long, T.; Telenti, A.; Mohney, R. P.; Small, K. S.; Bell, J. T.; Steves, C. J.; Valdes, A. M.; Spector, T. D.; Menni, C. The Fecal Metabolome as a Functional Readout of the Gut Microbiome. *Nat. Genet. 2018 506* **2018**, *50* (6), 790−795.

(25) Han, S.; Van Treuren, W.; Fischer, C. R.; Merrill, B. D.; DeFelice, B. C.; Sanchez, J. M.; Higginbottom, S. K.; Guthrie, L.; Fall, L. A.; Dodd, D.; Fischbach, M. A.; Sonnenburg, J. L. A Metabolomics Pipeline for the Mechanistic Interrogation of the Gut Microbiome. *Nature* **2021**, *595* (7867), 415−420.

(26) Shalon, D.; Culver, R. N.; Grembi, J. A.; Folz, J.; Treit, P. V.; Shi, H.; Rosenberger, F. A.; Dethlefsen, L.; Meng, X.; Yaffe, E.; Aranda-Díaz, A.; Geyer, P. E.; Mueller-Reif, J. B.; Spencer, S.; Patterson, A. D.; Triadafilopoulos, G.; Holmes, S. P.; Mann, M.; Fiehn, O.; Relman, D. A.; Huang, K. C. Profiling the Human Intestinal Environment under Physiological Conditions. *Nat. 2023 6177961* **2023**, *617* (7961), 581−591.

(27) Folz, J.; Culver, R. N.; Morales, J. M.; Grembi, J.; Triadafilopoulos, G.; Relman, D. A.; Huang, K. C.; Shalon, D.; Fiehn, O. Human Metabolome Variation along the Upper Intestinal Tract. *Nat. Metab.* **2023**, *5*, 777−788.

(28) Folz, J. S.; Shalon, D.; Fiehn, O. Metabolomics Analysis of Time-Series Human Small Intestine Lumen Samples Collected in Vivo. *Food Funct.* **2021**, *12* (19), 9405−9415.

(29) Stewart, A. K.; Foley, M. H.; Dougherty, M. K.; McGill, S. K.; Gulati, A. S.; Gentry, E. C.; Hagey, L. R.; Dorrestein, P. C.; Theriot, C. M.; Dodds, J. N.; Baker, E. S. Using Multidimensional Separations to Distinguish Isomeric Amino Acid−Bile Acid Conjugates and Assess Their Presence and Perturbations in Model Systems. *Anal. Chem.* **2023**, *95* (41), 15357−15366.

(30) Pang, Z.; Zhou, G.; Ewald, J.; Chang, L.; Hacariz, O.; Basu, N.; Xia, J. Using MetaboAnalyst 5.0 for LC−HRMS Spectra Processing, Multi-Omics Integration and Covariate Adjustment of Global Metabolomics Data. *Nat. Protoc. 2022 178* **2022**, *17* (8), 1735−1761.

(31) Bonini, P.; Kind, T.; Tsugawa, H.; Barupal, D. K.; Fiehn, O. Retip: Retention Time Prediction for Compound Annotation in Untargeted Metabolomics. *Anal. Chem.* **2020**, *92* (11), 7515−7522.

(32) Sumner, L. W.; Amberg, A.; Barrett, D.; Beale, M. H.; Beger, R.; Daykin, C. A.; Fan, T. W.-M.; Fiehn, O.; Goodacre, R.; Griffin, J. L.; Hankemeier, T.; Hardy, N.; Harnly, J.; Higashi, R.; Kopka, J.; Lane, A. N.; Lindon, J. C.; Marriott, P.; Nicholls, A. W.; Reily, M. D.; Thaden, J. J.; Viant, M. R. Proposed Minimum Reporting Standards for Chemical Analysis Chemical Analysis Working Group (CAWG) Metabolomics Standards Initiative (MSI). *Metabolomics* **2007**, *3* (3), 211−221.

https://doi.org/10.1021/acs.jproteome.4c00022
J. Proteome Res. 2024, 23, 2000−2012

(33) Cooper, B. T.; Yan, X.; Simón-Manso, Y.; Tchekhovskoi, D. V.; Mirokhin, Y. A.; Stein, S. E. Hybrid Search: A Method for Identifying Metabolites Absent from Tandem Mass Spectrometry Libraries. *Anal. Chem.* **2019**, *91* (21), 13924−13932.
(34) Nusbaum, D. J.; Sun, F.; Ren, J.; Zhu, Z.; Ramsy, N.; Pervolarakis, N.; Kunde, S.; England, W.; Gao, B.; Fiehn, O.; Michail, S.; Whiteson, K. Gut Microbial and Metabolomic Profiles after Fecal Microbiota Transplantation in Pediatric Ulcerative Colitis Patients. *FEMS Microbiol. Ecol.* **2018**, *94* (9), 133.
(35) Gotoh, K.; Sakaguchi, Y.; Kato, H.; Osaki, H.; Jodai, Y.; Wakuda, M.; Také, A.; Hayashi, S.; Morita, E.; Sugie, T.; Ito, Y.; Ohmiya, N. Fecal Microbiota Transplantation as Therapy for Recurrent Clostridioides Difficile Infection Is Associated with Amelioration of Delirium and Accompanied by Changes in Fecal Microbiota and the Metabolome. *Anaerobe* **2022**, *73*, No. 102502.
(36) Karu, N.; Deng, L.; Slae, M.; Guo, A. C.; Sajed, T.; Huynh, H.; Wine, E.; Wishart, D. S. A Review on Human Fecal Metabolomics: Methods, Applications and the Human Fecal Metabolome Database. *Anal. Chim. Acta* **2018**, *1030*, 1−24.
(37) Lamichhane, S.; Sundekilde, U. K.; Blædel, T.; Dalsgaard, T. K.; Larsen, L. H.; Dragsted, L. O.; Astrup, A.; Bertram, H. C. Optimizing Sampling Strategies for NMR-Based Metabolomics of Human Feces: Pooled vs. Unpooled Analyses. *Anal. Methods* **2017**, *9* (30), 4476−4480.
(38) Younes, M.; Aggett, P.; Aguilar, F.; Crebelli, R.; Dusemund, B.; Filipič, M.; Frutos, M. J.; Galtier, P.; Gott, D.; Gundert-Remy, U.; Kuhnle, G. G.; Lambré, C.; Lillegaard, I. T.; Moldeus, P.; Mortensen, A.; Oskarsson, A.; Stankovic, I.; Waalkens-Berendsen, I.; Woutersen, R. A.; Wright, M.; Boon, P.; Lindtner, O.; Tlustos, C.; Tard, A.; Leblanc, J. C. Refined Exposure Assessment of Polyethylene Glycol (E 1521) from Its Use as a Food Additive. *EFSA J.* **2018**, *16* (6), 1−17.
(39) Chaussade, S.; Minić, M. Comparison of Efficacy and Safety of Two Doses of Two Different Polyethylene Glycol-Based Laxatives in the Treatment of Constipation. *Aliment. Pharmacol. Ther.* **2003**, *17* (1), 165−172.
(40) Weaver, R.; Riley, R. J. Identification and Reduction of Ion Suppression Effects on Pharmacokinetic Parameters by Polyethylene Glycol 400. *Rapid Commun. Mass Spectrom.* **2006**, *20* (17), 2559−2564.
(41) Schymanski, E. L.; Jeon, J.; Gulde, R.; Fenner, K.; Ruff, M.; Singer, H. P.; Hollender, J. Identifying Small Molecules via High Resolution Mass Spectrometry: Communicating Confidence. *Environ. Sci. Technol.* **2014**, *48* (4), 2097−2098.
(42) Fiehn, O.; Robertson, D.; Griffin, J.; van der Werf, M.; Nikolau, B.; Morrison, N.; Sumner, L. W.; Goodacre, R.; Hardy, N. W.; Taylor, C.; Fostel, J.; Kristal, B.; Kaddurah-Daouk, R.; Mendes, P.; van Ommen, B.; Lindon, J. C.; Sansone, S. A. The Metabolomics Standards Initiative (MSI). *Metabolomics* **2007**, *3* (3), 175−178.
(43) Alpert, A. J. Hydrophilic-Interaction Chromatography for the Separation of Peptides, Nucleic Acids and Other Polar Compounds. *J. Chromatogr. A* **1990**, *499* (19), 177−196.
(44) Jandera, P.; Janás, P. Recent Advances in Stationary Phases and Understanding of Retention in Hydrophilic Interaction Chromatography. A Review. *Anal. Chim. Acta* **2017**, *967*, 12−32.
(45) McCalley, D. V. Understanding and Manipulating the Separation in Hydrophilic Interaction Liquid Chromatography. *J. Chromatogr. A* **2017**, *1523*, 49−71.
(46) Li, Y.; Kind, T.; Folz, J.; Vaniya, A.; Mehta, S. S.; Fiehn, O. Spectral Entropy Outperforms MS/MS Dot Product Similarity for Small-Molecule Compound Identification. *Nat. Methods* **2021**, *18*, 1524−1531.
(47) Koelmel, J. P.; Kroeger, N. M.; Gill, E. L.; Ulmer, C. Z.; Bowden, J. A.; Patterson, R. E.; Yost, R. A.; Garrett, T. J. Expanding Lipidome Coverage Using LC-MS/MS Data-Dependent Acquisition with Automated Exclusion List Generation. *J. Am. Soc. Mass Spectrom.* **2017**, *28* (5), 908−917.
(48) Kohler, I.; Verhoeven, M.; Haselberg, R.; Gargano, A. F. G. Hydrophilic Interaction Chromatography − Mass Spectrometry for Metabolomics and Proteomics: State-of-the-Art and Current Trends. *Microchem. J.* **2022**, *175*, No. 106986.
(49) Giddings, J. C. Two-Dimensional Separations: Concept and Promise. *Anal. Chem.* **1984**, *56* (12), 1258A−1270A.
(50) Gilar, M.; Olivova, P.; Daly, A. E.; Gebler, J. C. Orthogonality of Separation in Two-Dimensional Liquid Chromatography. *Anal. Chem.* **2005**, *77* (19), 6426−6434.
(51) Djoumbou Feunang, Y.; Eisner, R.; Knox, C.; Chepelev, L.; Hastings, J.; Owen, G.; Fahy, E.; Steinbeck, C.; Subramanian, S.; Bolton, E.; Greiner, R.; Wishart, D. S. ClassyFire: Automated Chemical Classification with a Comprehensive, Computable Taxonomy. *J. Cheminform.* **2016**, *8* (1), 1−20.
(52) Vangeenderhuysen, P.; Van Arnhem, J.; Pomian, B.; De Graeve, M.; De Commer, L.; Falony, G.; Raes, J.; Zhernakova, A.; Fu, J.; Hemeryck, L.Y.; Vanhaecke, L. Dual UHPLC-HRMS Metabolomics and Lipidomics and Automated Data Processing Workflow for Comprehensive High-Throughput Gut Phenotyping. *Anal. Chem.* **2023**, *95* (22), 8461−8468.
(53) Theriot, C. M.; Koenigsknecht, M. J.; Carlson, P. E.; Hatton, G. E.; Nelson, A. M.; Li, B.; Huffnagle, G. B.; Li, J. Z.; Young, V. B. Antibiotic-Induced Shifts in the Mouse Gut Microbiome and Metabolome Increase Susceptibility to Clostridium Difficile Infection. *Nat. Commun.* **2014**, *5*, 3114.
(54) Theriot, C. M.; Koenigsknecht, M. J.; Carlson, P. E.; Hatton, G. E.; Nelson, A. M.; Li, B.; Huffnagle, G. B.; Li, J. Z.; Young, V. B. Antibiotic-Induced Shifts in the Mouse Gut Microbiome and Metabolome Increase Susceptibility to Clostridium Difficile Infection. *Nat. Commun.* **2014**, *5*, 3114.
(55) Zhu, D.; Sorg, J. A.; Sun, X. Clostridioides Difficile Biology: Sporulation, Germination, and Corresponding Therapies for C. Difficile Infection. *Front. Cell. Infect. Microbiol.* **2018**, *8* (FEB), 29.
(56) Tam, J.; Icho, S.; Utama, E.; Orrell, K. E.; Gómez-Biagi, R. F.; Theriot, C. M.; Kroh, H. K.; Rutherford, S. A.; Borden Lacy, D.; Melnyk, R. A. Intestinal Bile Acids Directly Modulate the Structure and Function of C. Difficile TcdB Toxin. *Proc. Natl. Acad. Sci. U. S. A.* **2020**, *117* (12), 6792−6800.
(57) Thanissery, R.; Winston, J. A.; Theriot, C. M. Inhibition of Spore Germination, Growth, and Toxin Activity of Clinically Relevant C. Difficile Strains by Gut Microbiota Derived Secondary Bile Acids. *Anaerobe* **2017**, *45*, 86−100.
(58) Aguirre, A. M.; Yalcinkaya, N.; Wu, Q.; Swennes, A.; Tessier, M. E.; Roberts, P.; Miyajima, F.; Savidge, T.; Sorg, J. A. Bile Acid-Independent Protection against Clostridioides Difficile Infection. *PLOS Pathog.* **2021**, *17* (10), No. e1010015.
(59) Michel, A. M.; Borrero-de Acuña, J. M.; Molinari, G.; Ünal, C. M.; Will, S.; Derksen, E.; Barthels, S.; Bartram, W.; Schrader, M.; Rohde, M.; Zhang, H.; Hoffmann, T.; Neumann-Schaal, M.; Bremer, E.; Jahn, D. Cellular Adaptation of Clostridioides Difficile to High Salinity Encompasses a Compatible Solute-Responsive Change in Cell Morphology. *Environ. Microbiol.* **2022**, *24* (3), 1499−1517.
(60) Wilson, K. H.; Perini, F. Role of Competition for Nutrients in Suppression of Clostridium Difficile by the Colonic Microflora. *Infect. Immun.* **1988**, *56* (10), 2610−2614.
(61) Ramos, R. J.; Zhu, C.; Joseph, D. F.; Thaker, S.; LaComb, J. F.; Markarian, K.; Lee, H. J.; Petrov, J. C.; Monzur, F.; Buscaglia, J. M.; Chawla, A.; Small-Harary, L.; Gathungu, G.; Morganstern, J. A.; Yang, J.; Li, J.; Pamer, E. G.; Robertson, C. E.; Frank, D. N.; Cross, J. R.; Li, E. Metagenomic and Bile Acid Metabolomic Analysis of Fecal Microbiota Transplantation for Recurrent Clostridiodes Difficile and/or Inflammatory Bowel Diseases. *Med. Res. Arch.* **2022**.
(62) Robinson, J. I.; Weir, W. H.; Crowley, J. R.; Hink, T.; Reske, K. A.; Kwon, J. H.; Burnham, C. A. D.; Dubberke, E. R.; Mucha, P. J.; Henderson, J. P. Metabolomic Networks Connect Host-Microbiome Processes to Human Clostridioides Difficile Infections. *J. Clin. Invest.* **2019**, *129* (9), 3792−3806.
(63) Fletcher, J. R.; Erwin, S.; Lanzas, C.; Theriot, C. M. Shifts in the Gut Metabolome and Clostridium Difficile Transcriptome throughout Colonization and Infection in a Mouse Model. *mSphere* **2018**.

https://doi.org/10.1021/acs.jproteome.4c00022
J. Proteome Res. 2024, 23, 2000−2012

(64) Reed, A. D.; Fletcher, J. R.; Huang, Y. Y.; Thanissery, R.; Rivera, A. J.; Parsons, R. J.; Stewart, A. K.; Kountz, D. J.; Shen, A.; Balskus, E. P.; Theriot, C. M. The Stickland Reaction Precursor Trans −4-Hydroxy- l -Proline Differentially Impacts the Metabolism of Clostridioides Difficile and Commensal Clostridia. *mSphere* **2022**.
(65) Fletcher, J. R.; Pike, C. M.; Parsons, R. J.; Rivera, A. J.; Foley, M. H.; McLaren, M. R.; Montgomery, S. A.; Theriot, C. M. Clostridioides Difficile Exploits Toxin-Mediated Inflammation to Alter the Host Nutritional Landscape and Exclude Competitors from the Gut Microbiota. *Nat. Commun.* **2021**.
(66) Bremer, E.; Krämer, R. Responses of Microorganisms to Osmotic Stress. *Annu. Rev.* **2019**, *73*, 313−334.
(67) Dührkop, K.; Fleischauer, M.; Ludwig, M.; Aksenov, A. A.; Melnik, A. V.; Meusel, M.; Dorrestein, P. C.; Rousu, J.; Böcker, S. SIRIUS 4: A Rapid Tool for Turning Tandem Mass Spectra into Metabolite Structure Information. *Nat. Methods* **2019**, *16* (4), 299−302.
(68) Hoffmann, M. A.; Nothias, L. F.; Ludwig, M.; Fleischauer, M.; Gentry, E. C.; Witting, M.; Dorrestein, P. C.; Dührkop, K.; Böcker, S. High-Confidence Structural Annotation of Metabolites Absent from Spectral Libraries. *Nat. Biotechnol. 2022 403* **2022**, *40* (3), 411−421.
(69) Dührkop, K.; Nothias, L. F.; Fleischauer, M.; Reher, R.; Ludwig, M.; Hoffmann, M. A.; Petras, D.; Gerwick, W. H.; Rousu, J.; Dorrestein, P. C.; Böcker, S. Systematic Classification of Unknown Metabolites Using High-Resolution Fragmentation Mass Spectra. *Nat. Biotechnol.* **2021**, *39* (4), 462−471.
(70) Fukiya, S.; Arata, M.; Kawashima, H.; Yoshida, D.; Kaneko, M.; Minamida, K.; Watanabe, J.; Ogura, Y.; Uchida, K.; Itoh, K.; Wada, M.; Ito, S.; Yokota, A. Conversion of Cholic Acid and Chenodeoxycholic Acid into Their 7-Oxo Derivatives by Bacteroides Intestinalis AM-1 Isolated from Human Feces. *FEMS Microbiol. Lett.* **2009**, *293* (2), 263−270.
(71) Quinn, R. A.; Melnik, A. V.; Vrbanac, A.; Fu, T.; Patras, K. A.; Christy, M. P.; Bodai, Z.; Belda-Ferre, P.; Tripathi, A.; Chung, L. K.; Downes, M.; Welch, R. D.; Quinn, M.; Humphrey, G.; Panitchpakdi, M.; Weldon, K. C.; Aksenov, A.; da Silva, R.; Avila-Pacheco, J.; Clish, C.; Bae, S.; Mallick, H.; Franzosa, E. A.; Lloyd-Price, J.; Bussell, R.; Thron, T.; Nelson, A. T.; Wang, M.; Leszczynski, E.; Vargas, F.; Gauglitz, J. M.; Meehan, M. J.; Gentry, E.; Arthur, T. D.; Komor, A. C.; Poulsen, O.; Boland, B. S.; Chang, J. T.; Sandborn, W. J.; Lim, M.; Garg, N.; Lumeng, J. C.; Xavier, R. J.; Kazmierczak, B. I.; Jain, R.; Egan, M.; Rhee, K. E.; Ferguson, D.; Raffatellu, M.; Vlamakis, H.; Haddad, G. G.; Siegel, D.; Huttenhower, C.; Mazmanian, S. K.; Evans, R. M.; Nizet, V.; Knight, R.; Dorrestein, P. C. Global Chemical Effects of the Microbiome Include New Bile-Acid Conjugations. *Nat. 2020 5797797* **2020**, *579* (7797), 123−129.
(72) Foley, M. H.; Walker, M. E.; Stewart, A. K.; O'Flaherty, S.; Gentry, E. C.; Patel, S.; Beaty, V. V.; Allen, G.; Pan, M.; Simpson, J. B.; Perkins, C.; Vanhoy, M. E.; Dougherty, M. K.; McGill, S. K.; Gulati, A. S.; Dorrestein, P. C.; Baker, E. S.; Redinbo, M. R.; Barrangou, R.; Theriot, C. M. Bile Salt Hydrolases Shape the Bile Acid Landscape and Restrict Clostridioides Difficile Growth in the Murine Gut. *Nat. Microbiol. 2023 84* **2023**, *8* (4), 611−628.
(73) Wang, M.; Carver, J. J.; Phelan, V. V.; Sanchez, L. M.; Garg, N.; Peng, Y.; Nguyen, D. D.; Watrous, J.; Kapono, C. A.; Luzzatto-Knaan, T.; Porto, C.; Bouslimani, A.; Melnik, A. V.; Meehan, M. J.; Liu, W. T.; Crüsemann, M.; Boudreau, P. D.; Esquenazi, E.; Sandoval-Calderón, M.; Kersten, R. D.; Pace, L. A.; Quinn, R. A.; Duncan, K. R.; Hsu, C. C.; Floros, D. J.; Gavilan, R. G.; Kleigrewe, K.; Northen, T.; Dutton, R. J.; Parrot, D.; Carlson, E. E.; Aigle, B.; Michelsen, C. F.; Jelsbak, L.; Sohlenkamp, C.; Pevzner, P.; Edlund, A.; McLean, J.; Piel, J.; Murphy, B. T.; Gerwick, L.; Liaw, C. C.; Yang, Y. L.; Humpf, H. U.; Maansson, M.; Keyzers, R. A.; Sims, A. C.; Johnson, A. R.; Sidebottom, A. M.; Sedio, B. E.; Klitgaard, A.; Larson, C. B.; Boya, C. A. P.; Torres-Mendoza, D.; Gonzalez, D. J.; Silva, D. B.; Marques, L. M.; Demarque, D. P.; Pociute, E.; O'Neill, E. C.; Briand, E.; Helfrich, E. J. N.; Granatosky, E. A.; Glukhov, E.; Ryffel, F.; Houson, H.; Mohimani, H.; Kharbush, J. J.; Zeng, Y.; Vorholt, J. A.; Kurita, K. L.; Charusanti, P.; McPhail, K. L.; Nielsen, K. F.; Vuong, L.; Elfeki, M.; Traxler, M. F.; Engene, N.; Koyama, N.; Vining, O. B.; Baric, R.; Silva, R. R.; Mascuch, S. J.; Tomasi, S.; Jenkins, S.; Macherla, V.; Hoffman, T.; Agarwal, V.; Williams, P. G.; Dai, J.; Neupane, R.; Gurr, J.; Rodríguez, A. M. C.; Lamsa, A.; Zhang, C.; Dorrestein, K.; Duggan, B. M.; Almaliti, J.; Allard, P. M.; Phapale, P.; Nothias, L. F.; Alexandrov, T.; Litaudon, M.; Wolfender, J. L.; Kyle, J. E.; Metz, T. O.; Peryea, T.; Nguyen, D. T.; VanLeer, D.; Shinn, P.; Jadhav, A.; Müller, R.; Waters, K. M.; Shi, W.; Liu, X.; Zhang, L.; Knight, R.; Jensen, P. R.; Palsson, B.; Pogliano, K.; Linington, R. G.; Gutiérrez, M.; Lopes, N. P.; Gerwick, W. H.; Moore, B. S.; Dorrestein, P. C.; Bandeira, N. Sharing and Community Curation of Mass Spectrometry Data with Global Natural Products Social Molecular Networking. *Nat. Biotechnol.* **2016**, *34*, 828−837.
(74) GRUNDY, S. M.; AHRENS, E. H.; MIETTINEN, T. A. Quantitative Isolation and Gas−Liquid Chromatographic Analysis of Total Fecal Bile Acids. *J. Lipid Res.* **1965**, *6* (3), 397−410.
(75) Kakiyama, G.; Muto, A.; Takei, H.; Nittono, H.; Murai, T.; Kurosawa, T.; Hofmann, A. F.; Pandak, W. M.; Bajaj, J. S. A Simple and Accurate HPLC Method for Fecal Bile Acid Profile in Healthy and Cirrhotic Subjects: Validation by GC-MS and LC-MS. *J. Lipid Res.* **2014**, *55* (5), 978−990.
(76) Takei, H.; Narushima, S.; Suzuki, M.; Kakiyama, G.; Sasaki, T.; Murai, T.; Yamashiro, Y.; Nittono, H. Characterization of Long-Chain Fatty Acid-Linked Bile Acids: A Major Conjugation Form of 3β-Hydroxy Bile Acids in Feces. *J. Lipid Res.* **2022**, *63*, 100275.
(77) Lei, J.; Mahar, R.; Chang, M. C.; Collins, J.; Merritt, M. E.; Garrett, T. J.; Yost, R. A. Segmented Flow Strategies for Integrating Liquid Chromatography-Mass Spectrometry with Nuclear Magnetic Resonance for Lipidomics. *Anal. Chem.* **2022**, *95*, 53.

https://doi.org/10.1021/acs.jproteome.4c00022
J. Proteome Res. 2024, 23, 2000−2012